Accumulation of Phosphorylated α-Synuclein in Aging Human Brain

YUKO SAITO, MD, PHD, AKIKO KAWASHIMA, MSC, NYOKA N. RUBERU, MD, HIDEO FUJIWARA, MSC,
SHUNICHI KOYAMA, MD, MOTOJI SAWABE, MD, PHD, TOMIO ARAI, MD, PHD, HIROSHI NAGURA, MD,
HIROSHI YAMANOUCHI, MD, PHD, MASATO HASEGAWA, PHD, TAKESHI IWATSUBO, MD, PHD,
AND SHIGEO MURAYAMA, MD, PHD

Abstract. α-Synuclein in Lewy bodies (LBs) is phosphorylated at Ser129. We raised monoclonal and polyclonal antibodies to this phosphorylation site (psyn) and examined 157 serial autopsy brains from a geriatric hospital. Anti-psyn immunoreactivity was observed in 40 of these cases (25.5%). Immunohistochemistry revealed 4 novel types of pathology: diffuse neuronal cytoplasmic staining (pre-LB); neuropil thread-like structures (Lewy threads); dot-like structures similar to argyrophilic grains (Lewy dots); and axons in the white matter (Lewy axons). This novel pathology was abundantly present around LBs and also involved the limbic subcortical white matter, the cerebral cortical molecular layer, and the spongiform changes of the medial temporal lobe associated with cases of dementia with LBs (DLB). The phosphorylated α-synuclein was limited to the temporal lobe in cases of Parkinson disease, spread from the temporal lobe to the frontal lobe in cases of DLB transitional form and further spread to the parietal and occipital lobes in DLB neocortical form. Our findings suggest that LB-related pathology initially involves the neuronal perikarya, dendrites, and axons, causes impairment of axonal transport and synaptic transmission, and later leads to the formation of LBs, a hallmark of functional disturbance long before neuronal cell death.

Key Words: α-Synucleinopathy; Axon; Dementia with Lewy bodies; Immunohistochemistry; Parkinson disease; Synapse.

INTRODUCTION

Lewy body (LB)-related pathology was originally recognized in the brains of patients with Parkinson disease. Since it was discovered that ubiquitin (1) and α-synuclein (2, 3) are components of LBs, the locations of LB-related pathology and the corresponding specific neurological abnormalities have received considerable attention. Involved sites include the peripheral autonomic nervous system in cases with autonomic failure (4), the dorsal motor nucleus of the vagus nerve in cases with dysphagia (5), and the limbic system and neocortex in cases with cognitive decline (i.e. dementia with Lewy bodies [DLB]) (6). The severity of clinical abnormalities in these cases parallels the number of LBs (7) rather than neuronal cell loss (8), especially in cases with DLB neocortical form.

Recent immunohistochemical studies with anti-α-synuclein antibodies suggest that the dorsal motor nucleus of the vagus is the initial site of involvement in Parkinson disease (9). In contrast, α-synuclein-positive structures preferentially localize in the amygdala in familial (10) and sporadic (11) Alzheimer disease (AD). Further clarification of the relationship between these 2 reported types of α-synucleinopathy has been difficult, because α-synuclein is a normal constituent of presynaptic structures (12), and interpretation of abnormal accumulations based on staining intensity may be influenced by the conditions of staining or fixation.

We recently reported that the α-synuclein accumulated in LBs (13) is phosphorylated at Ser129, and that a polyclonal anti-phosphorylated α-synuclein antibody (anti-PSer129) produced strong staining of LBs and Lewy neurites (13). We have now raised a monoclonal antibody (psyn#64) that specifically recognizes this phosphorylation site. Immunohistochemistry with this highly specific monoclonal antibody produces intense staining of LBs and Lewy neurites without staining normal presynaptic structures.

In the current study, we examined serial autopsy brains from an aging population to assess the progression of the 2 reported types of LB-related α-synucleinopathy. We also correlated the morphological changes with the severe functional impairment that occurs prior to cell loss in LB-related cognitive decline.

From Department of Neuropathology, Tokyo Metropolitan Institute of Gerontology (YS, NNR, SK, SM), Tokyo, Japan; Department of Neuropathology and Neuroscience, Graduate School of Pharmaceutical Science (AK, HF, TI), University of Tokyo, Tokyo Japan; Department of Neurology, Division of Neuroscience, Graduate School of Medicine (NNR), University of Tokyo, Tokyo, Japan; Department of Geriatric Medicine (SK), Tokyo Medical University, Tokyo, Japan; Departments of Pathology (MS, TA) and Neurology (HN, HY), Tokyo Metropolitan Geriatric Hospital, Tokyo, Japan; Department of Molecular Neurobiology (MH), Tokyo Institute of Psychiatry, Tokyo, Japan.

Correspondence to: Shigeo Murayama, MD, PhD, Department of Neuropathology, Tokyo Metropolitan Institute of Gerontology, 35-2 Sakaecho, Itabashi-ku, Tokyo 173-0015, Japan. E-mail: smurayam@tmig.or.jp

Sources of support: Foundation of Tokyo Metropolitan Institute of Gerontology.
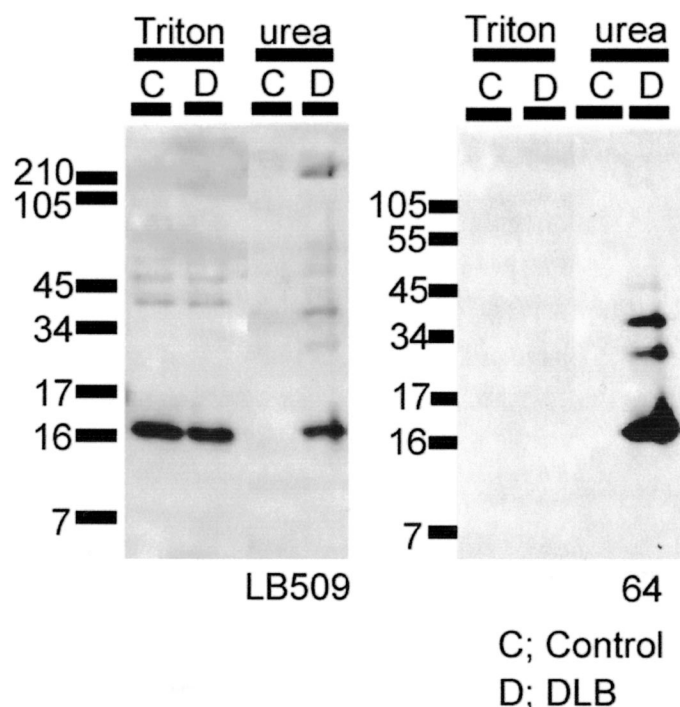
MATERIALS AND METHODS

Tissue Source

One hundred and fifty-seven serial autopsy brains from Tokyo Metropolitan Geriatric Hospital (TMGH) were studied in the present work. The patients' ages ranged from 48 to 100 years. The mean age was 81.1 ± 8.6 years and the male to female ratio was 89:68.

Fig. 1. Western blot analysis of α-synuclein differentially extracted with Triton X-100 (Triton), Sarkosyl, or urea from cerebral cortices of a patient with DLB, neocortical form (Case 4) and a normal control individual probed with LB509 (left panel) or psyn#64 (right panel). Sarkosyl soluble fractions that did not contain detectable amounts of α-synuclein are not shown. Molecular weight markers are shown in kilodaltons at the left side of the panels. A ~15 kDa polypeptide, labeled by LB509 (3), was detected in TX-soluble fractions of DLB and normal control brains and represents normal α-synuclein, as previously reported (13). A major ~15 kDa polypeptide and additional minor higher molecular weight polypeptides were specifically detected by LB509 in Sarkosyl-insoluble, urea-soluble fractions from DLB cortices. Monoclonal antibody psyn#64 did not label TX-soluble α-synuclein, but strongly reacted with the urea-soluble α-synuclein in DLB brains.

Neuropathology

Sections of the right substantia nigra, amygdala, anterior hippocampus and frontal, temporal, parietal, and occipital lobes were fixed in 4% paraformaldehyde for 48 hours and embedded in paraffin. The left half of the brain was fixed in 20% neural buffered formalin (Wako, Osaka, Japan) for 7 to 13 days and representative areas were embedded in paraffin.

Six-μm-thick sections were stained with hematoxylin and eosin (H&E) and by the Klüver-Barrera method. Selected sections were examined with modified methenamine and Gallyas-Braak silver staining for senile changes, with Congo red staining for amyloid deposition, and with elastica Masson staining for vascular changes.

Preparation and Characterization of Anti-Phosphorylated α-Synucliein (psyn) Monoclonal Antibody (psyn#64)

Anti-psyn monoclonal antiobody (psyn#64) was raised against a synthetic peptide corresponding to residues 124–134 of human α-synuclein containing phosphoserine at position 129 and screened by ELISA. For the characterization of the antibody, neocortex from the medial temporal lobe of brains with DLB neocortical form and of normal control brains from the present autopsy series were differentially extracted as previously described (13), with some modifications. Briefly, the neocortices were directly homogenized in 1% Triton X-100 (TX) containing protease inhibitors (instead of Tris saline) and then extracted with Sarkosyl and urea. TX- or urea-soluble fractions, in which normal and deposited α-synuclein is extracted, respectively, were separated by SDS-PAGE and analyzed by immunoblotting with LB509 (3) or psyn#64 as primary antibodies. In addition, the immunoreactivity was confirmed by immunoblot with nonphosphorylated recombinant human α-synuclein and α-synuclein phosphorylated in vitro by casein kinase 2, which specifically phosphorylates Ser129 (3) (A.K., H.F., and T.I., unpublished observation).

Immunohistochemistry

Six-μm-thick serial sections were obtained from paraffin blocks and immunohistochemically stained using a Ventana 20NX autostainer (Ventana, Tucson, AZ) for single or double immunolabeling as previously described (14). Two antibodies specific for phosphorylated α-synuclein (mouse monoclonal antibody psyn#64 and polyconal antibody anti-Pser129 [13]) were used. In addition, other antibodies against α-synuclein (LB509, monoclonal [3] & and S1, recognizing the C terminus [a kind gift from Dr. Y. Ihara]); phosphorylated tau (AT8, monoclonal, Innogenetics, Temse, Belgium); Aβ11-28 (12B2, monoclonal, IBL, Maebashi, Japan); ubiquitin (polyclonal, Sigma-Aldrich, St. Louis, MO); glial fibrillary acidic protein (GFAP, polyclonal, DAKO, Carpinteria, CA); and HLA-DR (CD68, monoclonal, DAKO) were also used. The sections were pretreated with 99% formic acid for 5 min for psyn#64 and anti-Aβ, or heated in a microwave oven (Nisshin EM, Tokyo, Japan) for 10 min in citrate buffer before incubation with LB509, CD68, or anti-ubiquitin antibody. Areas selected for staining with psyn#64 included all of the paraformaldehyde-fixed tissues, as well as areas from the formalin-fixed tissues recommended by the consensus guidelines for dementia with Lewy bodies (DLB) (6) (lumbar, thoracic, and cervical spinal cord, medulla oblongata at the level of the dorsal motor nucleus of the vagus nerve, upper pons at the level of the locus ceruleus, midbrain, and basal ganglia, anterior cingulate and entorhinal cortex, amygdala, and second frontal, temporal and supramarginal gyri).

Phosphorylated α-synuclein was detected in dendrites or axons with confocal double immunofluorescence using anti-Pser129 combined with anti-MAP2 (HM2, monoclonal, Sigma, St. Louis, MO) or anti-phosphorylated neurofilament (SMI 31, monoclonal, Sternberger Immunochemicals, Bethesda, MA) antibody. Primary antibodies were visualized with anti-rabbit Alexa 568 Fluor™ and anti-mouse IgG Alexa 488™ (Molecular Probes, Eugene, OR) using a confocal laser microscope (BioRad, Hercules, CA). SMI 31 was diluted up to 1:10,000 in order to avoid possible cross-reaction with phosphorylated tau protein.

Evaluation of Lewy Body-Related Neuropathology

The brains were initially evaluated and their LB scores calculated from sections stained with H&E and anti-ubiquitin immunohistochemistry, as recommended by the consensus guidelines for DLB (6). The presence of LB-related pathology was
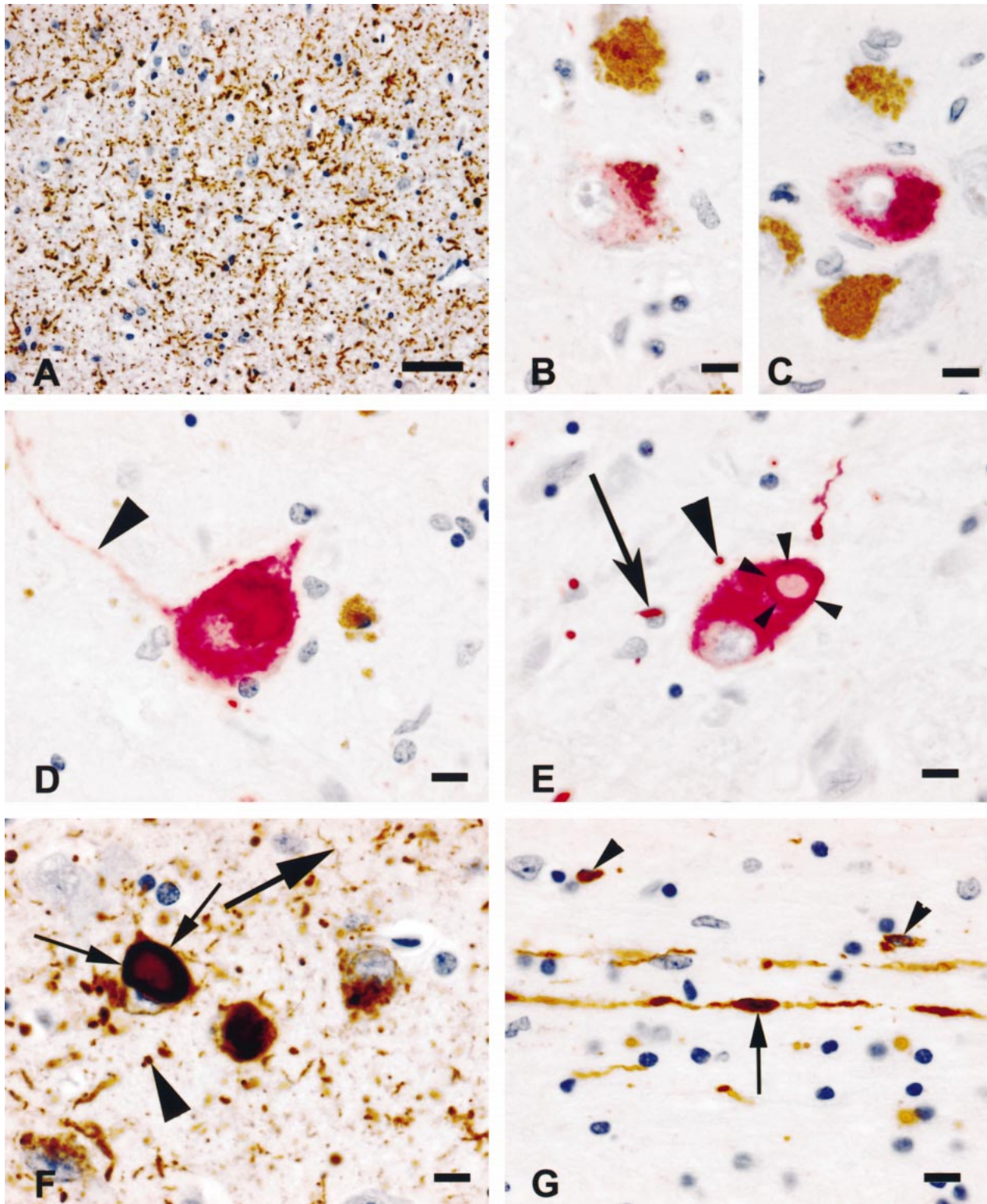
Fig. 2. Novel morphological alterations visualized by immunohistochemistry with anti-phosphorylated α-synuclein (psyn) antibodies. **A:** Numerous dots and threads within the spongiosis in the entorhinal cortex (case 1, bar = 50 μm). **B–E:** Possible morphologic progression in the formation of LBs in melanin-containing neurons of the substantia nigra (Ventana red staining for alkaline phosphatase, bars = 10 μm). **B:** Weak cytoplasmic staining (case 13). **C:** Diffuse cytoplasmic staining (case 14). **D:** Focal cytoplasmic aggregate and positive axon (arrowhead) (case 13). **E:** Typical lamellar staining (small arrowheads), consistent with LBs, associated with neuropil dots (large arrowhead) and a glial inclusion (arrow) (case 6). **F:** Anti-psyn-immunoreactive threads (thick arrow) and dots (arrowhead) with cortical LBs (thin arrows) in the entorhinal cortex (stained with diaminobenzidine) (case 2). **G:** Axons in the white matter of the amygdala (fibrae amygdalofugal) with focal swellings (arrow), positive for anti-psyn antibodies. Anti-psyn-immunoreactive glial inclusions are also visible (arrowheads, case 2).
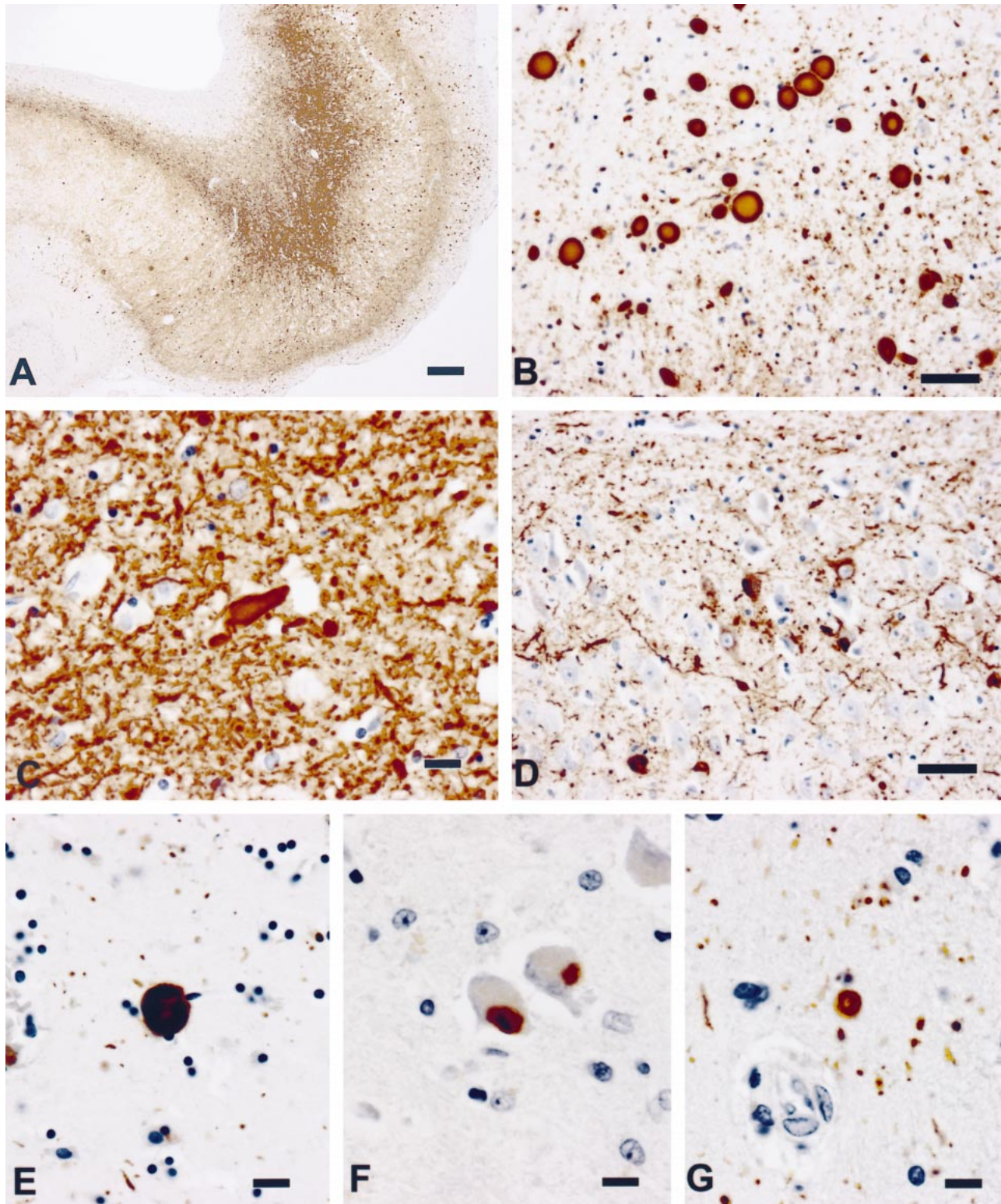
Fig. 3. Morphological alterations visualized by immunohistochemistry with anti-phosphorylated α-synuclein (psyn) antibodies. **A:** Prominent positive staining in the anterior alveus (bar = 0.25 mm, case 2). **B:** Clustered thick neurites in the molecular layer of the anterior subiculum (bar = 50 μm, case 2). **C:** Higher magnification of the alveus shown in (**A**), showing numerous axons with focal thickening (bar = 10 μm, case 2). **D:** Intracytoplasmic neuronal inclusions with neuritic threads and dots in CA2 and CA3 (bar = 50 μm, case 2). **E:** A large immunoreactive spheroid in the dorsomedial putamen (bar = 10 μm, case1). **F:** Neuronal intracytoplasmic inclusions in the inferior olivary nucleus (bar = 10 μm, case from stage 1B). **G:** Lewy dots, threads, and globules in the molecular layer of the striated cortex (bar = 15 μm, case 1).

immunohistochemically confirmed using anti-α-synuclein antibodies. Sections were then stained for phosphorylated α-synuclein with psyn#64, and based on this staining, a new LB score was calculated using the same criteria referenced above. Selected sections were also stained with polyclonal anti-psyn antibody (13) to confirm the results obtained with monoclonal psyn#64. Small pieces of brain with abundant LB-related pathology were directly fixed in 2.5% glutaraldehyde, postfixed in 1% osmium tetroxide, embedded in epon, and examined in an electron microscope (Hitachi 7500, Hitachi, Japan).

RESULTS

Neuropathology

The 157 serial autopsy brains examined here included 47 cases of neurodegenerative disorders: 15 cases of AD, 13 cases of dementia with grains (DG), 4 cases of DLB neocortical form, 5 cases of DLB transitional form, 2 cases of Parkinson disease, 3 cases of progressive supranuclear palsy (PSP), 1 case of corticobasal degeneration, 1 case of neurofibrillary tangle-predominant form of dementia (NFTD), 1 case of PSP plus DG, 1 case of NFTD plus DG, and 1 case of AD plus DG. All 5 cases with DLB transitional form were categorized as Parkinson disease with dementia, according to McKeith et al (i.e. the onset of dementia was more than 1 year later than the development of parkinsonism) (6, 15). In 3 of the 15 AD cases, LBs were preferentially present in the amygdala; they were abundant in 2 cases and scattered in the third. One case was consistent with LB-related dysphagia (5), with LBs and gliosis preferentially involving the dorsal motor nucleus of the vagus.

Based on examination with H&E staining and immunohistochemistry with anti-ubiquitin antibody, the 157 brains were classified into the following 5 categories: Stage 0: no LBs (128 cases); Stage I: scattered LBs without cell loss (9 cases); Stage II: abundant LBs with macroscopic loss of pigmentation in substantia nigra and locus ceruleus and/or gliosis demonstrated by GFAP immunohistochemistry in the areas containing LBs but without attributable parkinsonism or dementia (9 cases); Stage III: Parkinson disease (2 cases); Stage IV: DLB, transitional form (5 cases); and Stage V: DLB, neocortical form (4 cases).

Characterization of Anti-Phospho-α-Synuclein (psyn) Antibody

Western blotting of the differential extracts from DLB and control brains revealed a ~15 kDa polypeptide that was labeled by a human-specific anti α-synuclein antibody (LB509) (3). The polypeptide was detected in TX-soluble fractions from DLB and normal control brains and represents normal α-synuclein, as previously reported (13) (Fig. 1). A major ~15 kDa polypeptide and a minor additional higher molecular weight polypeptide, which may correspond to ubiquitinated α-synuclein species

(16), were detected by LB509 in Sarkosyl-insoluble, urea-soluble fractions from DLB cortices. Monoclonal antibody (mAb) psyn#64 did not label TX-soluble α-synuclein, but strongly reacted with the urea-soluble α-synuclein in DLB brains in an identical pattern to that observed using a phosphorylated Ser129-specific polyclonal antibody, (anti-PSer129) (3). Given that urea-soluble α-synuclein in DLB brains is highly phosphorylated at Ser129 and Tris/TX-soluble normal α-synuclein is not (3), the data are consistent with mAb psyn#64 reacting similarly to anti-PSer129, with the phosphorylation-dependent epitope around PSer129 of α-synuclein. On Western blotting of recombinant human α-synuclein, mAb psyn#64 recognized α-synuclein phosphorylated at Ser129 by casein kinase 2 (data not shown) but did not recognize nonphosphorylated α-synuclein.

Anti-Phospho-α-Synuclein (psyn) Immunopathology

Immunohistochemical staining with anti-α-synuclein (LB509 and S1) antibodies improved both the specificity and the sensitivity for LB-related pathology, as compared to anti-ubiquitin immunohistochemistry, but was seriously complicated by diffuse staining of the background with a synaptic, cytoplasmic, or axonal pattern. The background staining was especially pronounced in paraformaldehyde-fixed sections. Occasional spheroids in the amygdala and zona reticulata of the substantia nigra were also moderately immunoreactive with LB509 and S1.

In contrast, immunostaining with mAb psyn#64 did not produce background staining or anti-α-synuclein-immunoreactive spheroids. The mAb did reveal, however, positively staining Lewy dots (Fig. 2A, E, F) and Lewy threads (Fig. 2A, F) in association with LBs (Fig. 2E, F). These immunopositive dots and threads were best visualized in paraformaldehyde-fixed tissues but could also be detected in buffered-formalin-fixed tissues. Focal enlargement along the course of threads, which corresponded to Lewy neurites in adjacent anti-nonphosphorylated α-synuclein-stained sections, was frequently seen (Fig. 3D). The process of LB formation in pigmented neurons of the substantia nigra appeared to progress from faint (Fig. 2B) or intense (Fig. 2C) diffuse cytoplasmic staining (pre-LB) to single or multiple (Fig. 2D) focal cytoplasmic aggregates (corresponding to pale bodies) to typical positive rings with negative cores (corresponding to brainstem-type LBs) (Fig. 2E). Cortical LBs showed a similar process of progression from focal cytoplasmic accumulations of the epitope to round inclusions (Fig. 2F) with or without central pallor. Immunoreactive glial inclusions were occasionally observed among these neuronal lesions (Fig. 2E, G).

Anti-psyn immunohistochemistry also revealed intense immunoreactivity in the alveus in the subcortical area of the anterior subiculum (Fig. 3A, C), where abundant cortical LBs were present. Additionally, there was staining

in the white matter around the amygdala (Fig. 2G) and in the subcortical white matter of the anterior cingulate gyrus.

With confocal microscopy, anti-psyn immunoreactivity in the white matter was almost exclusively colocalized with the epitope of SMI 31 (Fig. 4A–C). In contrast, Lewy dots and threads in the gray matter were partially colocalized with the epitope of anti-MAP2 (Fig. 4D–F) or SMI 31 (data not shown).

Anti-psyn-immunoreactive structures were observed in 11 of the original Stage 0 cases, preferentially in the dorsal motor nucleus of the vagus and medullary reticular formation in 9 cases and in the amygdala in 2 cases (1 AD case and 1 cognitively normal case with grains (CNG) (14). Five of these 11 cases contained only Lewy dots and threads, but no perikaryal immunoreactivity (4 cases with immunoreactivity in the dorsal motor nucleus of vagus or medullary reticular formation and 1 case of AD with immunoreactivity in the amygdala). We included the 6 cases with perikaryal pre-LBs in a new Stage 1 and categorized the 5 cases with only threads and dots into a new Stage 0.5 (Table 1).

Thirteen of the 15 cases that were newly classified as Stage I with anti-psyn immunohistochemistry had positive staining most prominent in the medulla oblongata. The immunoreactivity was exclusively there in 2 cases, extended to the substantia nigra in 4 cases, and extended to the limbic structure in 7 cases. The remaining 2 cases had AD and showed neuronal intracytoplasmic staining exclusively in the amygdala. Some cases also showed focal aggregates of anti-psyn epitope in the inferior olivary nucleus (Fig. 3F), along with positive dots and threads in the dentate nucleus.

The original Stage II cases were newly subclassified into 2 groups: limbic (IIL, 4 cases), and neocortical variant (IIN, 5 cases), based on the new LB scores calculated with anti-psyn immunohistochemistry. Tables 2A and 2B summarize the cases in the original categories II-V based on examination with H&E and anti-ubiquitin antibody. Two AD cases (Cases 14 and 17 that had preferential involvement of the amygdala were classified into IIL (Case 17) and IIN (Case 14) and showed minor but not negligible positive immunoreactivity in the substantia nigra and dorsal motor nucleus of the vagus. These 2 AD cases contained anti-psyn-immunoreactive neuritic plaques and tangles in the amygdala, entorhinal cortex, and prosubiculum. The colocalization of the epitope of phosphorylated tau and psyn was frequent in the sections immunostained for both psyn#64 and AT8 (data not shown). One case of PSP also had preferential involvement of the amygdala, although anti-psyn-immunoreactivity was detected in all areas showing tauopathy, including the posterior horn of the spinal cord (17). In the amygdala, AT8-immunoreactive threads outnumbered psyn#64-immunoreactive threads and were rarely colocalized together in double-immunostained sections (data not shown). All cases of Stages IIL and IIN showed many LBs and Lewy neurites associated with dots in the transentorhinal area, as well as many Lewy neurites and pre-LBs in CA2 and CA3. Thick neurites, which were strongly immunoreactive with anti-psyn, clustered in the molecular layer of the anterior subiculum,. These thick neurites were most prominent in Stage V cases (Fig. 3B), but they were also seen in 1 of 4 cases of Stage IIL and all cases of Stage IIN. Some of these neurites were identified as intraneuritic LBs in the adjacent H&E-stained sections.

Stage III cases presented with definite limbic pathology involving the transentorhinal area, CA2, CA3, and amygdala. The clustered thick Lewy neurites in the molecular layer of the anterior subiculum were seen in all Stage III cases and were more conspicuous than in the Stage II cases. The involved temporal neocortex had numerous cortical LBs and neurites surrounded by dots and threads. Lesions involving hippocampal CA2 and CA3 were observed in all Stage III cases. The lesions gradually decreased in severity from frontal to parietal cortex, although number of anti-psyn-immunoreactive LBs or intraneuronal aggregates of psyn-immunoreactivity in parietal cortex were still sufficiently numerous for a score of 2, based on the published consensus guidelines (6).

Stage IV cases showed considerable anti-psyn immunoreactive structures in frontal neocortex, including the molecular layer, and in temporal neocortex. There was moderate immunoreactivity in the parietal cortex and mild immunoreactivity in the occipital cortex and striatum. The entorhinal and transentorhinal cortex showed spongiosis associated with numerous Lewy dots and accompanied by psyn-immunoreactive tangles. Approximately 10% of these tangles were also AT8-immunoreactive in double-immunostained sections (data not shown). The lesions in hippocampal CA2 and CA3 were more severe than those in Stage III cases.

Stage V cases showed more widespread neocortical involvement by anti-psyn immunoreactive structures and by degeneration in the limbic system. The lesions in CA2 and CA3 (Fig. 3D) and the spongiosis with numerous Lewy dots in the entorhinal and transentorhinal areas were more conspicuous in Stage V than Stage IV. Psyn-immunoreactive tangles were also more frequent in Stage IV. Scattered neuropil threads, which were immunoreactive for both AT8 and psyn#64, were present in double-immunostained sections (data not shown). The lesions were also more prominent in Stage V than in Stage IV in the cingulate gyrus, insular cortex and entire medial temporal lobe, and frontal and parietal cortex. Numerous Lewy dots were seen in the putamen, with a ventrolateral to dorsomedial gradient (Fig. 3E). Abundant Lewy dots and threads were also detected in the molecular layer of the affected cortical structures,
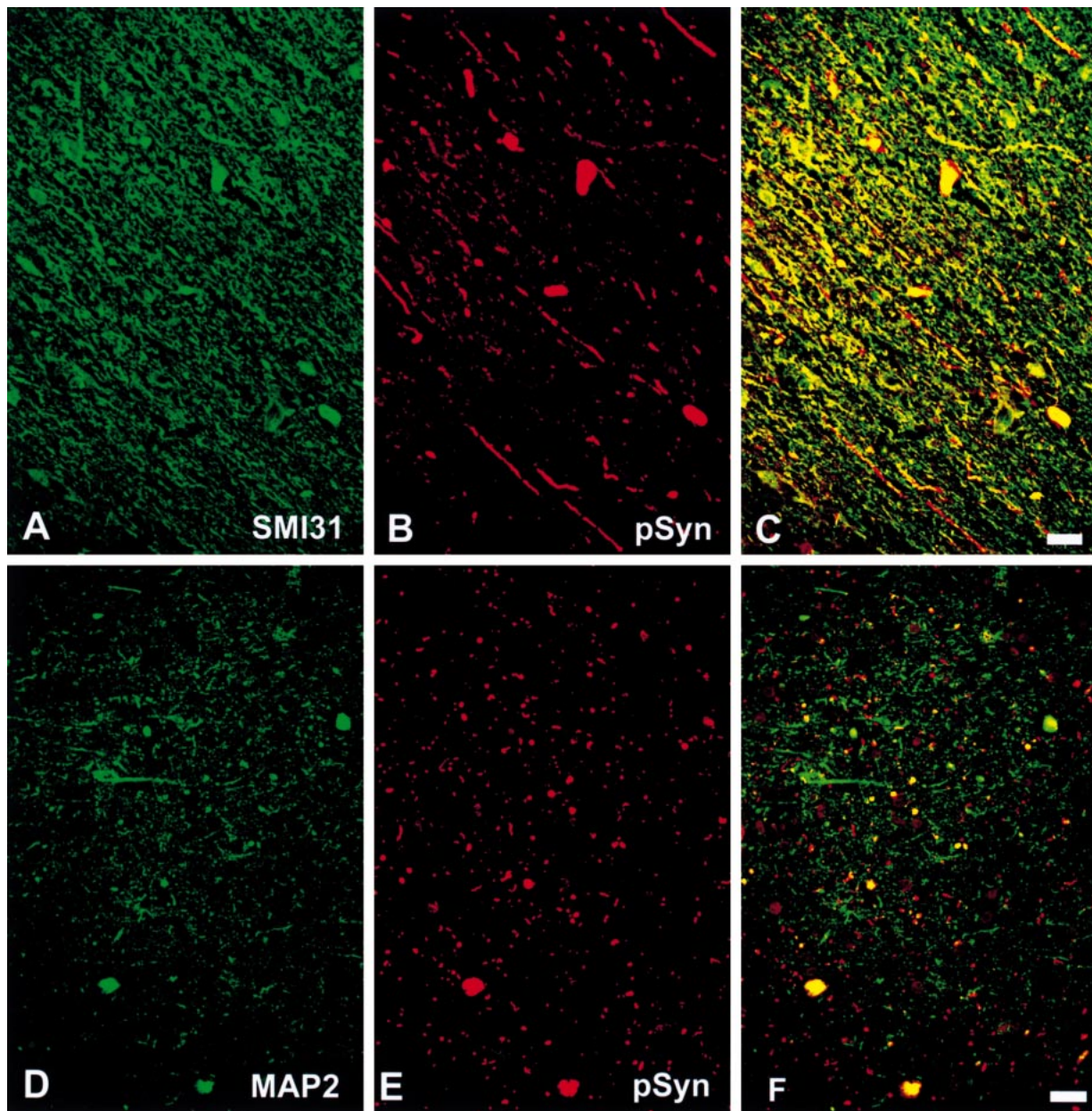
Fig. 4. Axonal and somatodendritic localization of phosphorylated α-synuclein. Sections of amygdala were double immunostained with polyclonal anti-phosphorylated -synuclein antibody (anti-PSer129) and with anti-phosphorylated neurofilament (SMI 31) (**A–C**) or anti-MAP2 (HM-2) (**D–F**). The primary antibodies were visualized with anti-rabbit Alexa 568 Fluor™ (red) and anti-mouse IgG Alexa 488™ (green) (Case 2). **A–C:** Confocal image of the white matter of the amygdala (the same area as Fig. 2F). The epitope of anti-Pser129 (red) is almost exclusively colocalized with that of SMI 31 (green). Anti-Pser129-immunoreactive axonal swellings are scattered. **D–F:** In the amygdala proper, some anti-Pser129-immunoreactive dots and threads (red) are colocalized with the epitope of anti-MAP2 antibody (green). **A, D:** Alexa 488 (green) for phosphorylated neurofilament (**A**) or MAP2 (**D**). **B, E:** Alexa 568 (red) for polyclonal phosphorylated α-synuclein, anti-Pser129. **C, F:** Merged views for (**A/B**) and (**D/E**). Scale bar = 20 μm.

including the occipital cortex (Fig. 3G). In the sections double-immunostained for both psyn#64 and anti-Aβ 11–28, almost all senile plaques contained anti-psyn-immunoreactive dystrophic neurites in the areas where the immunoreactivity with anti-psyn was abundant. Although very small in number, some amyloid cores appeared to contained the epitope of psyn.

Electron microscopic observation of the molecular layer of the anterior subiculum confirmed the presence of intraneuritic Lewy bodies. Ultrastructurally, the Lewy

TABLE 1
Early Lewy Body-Related Pathology Detected with Anti-Phosphorylated α-Synuclein Immunohistochemistry

Age (yr)	Sex	Neurological diagnosis	Pathological diagnosis	Distribution and extent					Original staging of Lewy body
				DMNX	RF	LC	SN	Amy	
Stage 0.5									
93	F	Dementia	DG	+−	−	+−	−	−	0
69	M	Unremarkable	Unremarkable	−	+−	−	+−	−	0
98	F	Dementia	DG	+−	+−	−	+−	+−	0
76	M	Unremarkable	Unremarkable	+−	+−	+−	+−	+−	0
86	M	AD	AD	−	−	−	−	+−	0
Stage I									
73	F	CVD	CVD	+	−	−	−	−	0
86	M	Unremarkable	Unremarkable	+	+	+−	−	+−	0
88	F	Hepatic coma	Unremarkable	+	+	−	+	+−	0
78	F	Dementia	DG/ NFTD	+	+	−	+−	+−	0
94	F	CVD s/o	CVD	+−	+	++	−	++	0
72	M	Unremarkable	CNG	−	+−	−	−	+	0
70	M	Unremarkable	Unremarkable	+−	+	++	+	+−	I
69	M	CVD, dementia	VD	++	+	++	+	+−	I
84	F	Unremarkable	Unremarkable	++	++	++	++	++	I
82	M	Unremarkable	CVD	++	++	++	++	+	I
78	M	Unremarkable	Unremarkable	+	+	++	+	+	I
80	M	Unremarkable	Unremarkable	++	+	+	+	++	I
78	M	Dementia	DG/ CVD	+	++	−	+	++	I
98	M	AD	AD	+−	−	−	+−	+	I
78	M	AD	AD	+−	+−	−	−	+	I

Abbreviations: DMNX, dorsal motor nucleus of vagus nerve; RF, reticular formation in the medulla oblongata; LC, locus ceruleus; SN, substantia nigra; Amy, amygdala; DG, dementia with grains; AD, Alzheimer disease; CVD, cerebrovascular disease; NFTD, neurofibrillary tangle-predominant form of dementia; CNG: cognitively normal case with grains (14); and VD, vascular dementia. Extent of antiphosphorylated α-synuclein immunoreactive structures are as follows: −, none; +−, dots and threads only; +, intraneuronal (perikaryal) presence of the epitope; ++, dense aggregates of the epitope in the neuronal cytoplasm.

bodies presented as large spherical amorphous cores of high electron density surrounded by meshworks of granulofilamentous profiles (not illustrated).

DISCUSSION

The present study revealed 4 new findings: 1) phosphorylation of α-synuclein (psyn) occurred in about one fourth of the aged population; 2) anti-psyn immunocytochemistry allowed novel visualization of pre-LBs as well as Lewy threads, dots, and axons; 3) α-synucleinopathy begins in the medulla oblongata if it is an independent disease process, or in the amygdala if associated with AD; and 4) severe neocortical involvement by psyn is present in the medial temporal lobe in Parkinson disease, extends to the frontal lobe in DLB transitional form, and additionally involves the parietal and occipital lobes in DLB neocortical form.

We believe that our autopsy series is reasonably representative of the general older population in Japan. The 157 brains we examined are from a serial autopsy series at TMGH. This is one of the oldest and largest public geriatric hospitals in Japan, with 900 outpatients daily and a 700-bed ward. Every effort is made to secure postmortem neuropathological examinations on all patients dying at TMGH, whether or not a neurological disease was diagnosed antemortem. The autopsy rate was 32% during the period of this study.

Anti-psyn immunohistochemistry resulted in better visualization of previously reported LB-related pathology, except in a few anatomical loci such as the inferior olivary nucleus and occipital cortex. Using this more specific and sensitive marker, we found that 25 percent of the cases in our serial autopsy series had LB-related pathology. The limbic pathology specifically linked to DLB was detected in apparently presymptomatic cases, suggesting that phosphorylation of α-synuclein at Ser129 represents a pathological change that precedes LB-related neuronal degeneration. The pre-LBs, Lewy threads, and Lewy dots detected with anti-psyn immunohistochemistry are morphologically analogous to the pretangles, neuropil threads, and argyrophilic grains (18) detected with anti-phosphorylated tau immunohistochemistry. The Lewy threads were thinner and shorter than the Lewy neurites detected with anti-ubiquitin or anti-α-synuclein

TABLE 2A
Clinical Profiles of the Cases Showing Lewy Body-Related Neuronal Degeneration

Case	Age (yr)	Sex	Neurological diagnosis	CDR	PA	Dementia	Pathological diagnosis
1	85	M	PD+AD	3	10 yr	2 yr	DLBN
2	83	F	DLB	1	(–)	>2 yr	DLBN
3	92	F	Senile dementia	3	(–)	>2 yr	DLBN
4	77	M	DLB	3	2 yr	6 yr	DLBN
5	88	M	PD+dementia	1	11 yr	4 yr	DLBT
6	85	F	PD+dementia	1	19 yr	5 yr	DLBT
7	85	M	Drug-induced PA	1	>1 yr	n.d.	DLBT
8	86	F	PD+dementia	2	20 yr	1.75 yr	DLBT
9	79	F	PD+dementia	2	8 yr	>1 yr	DLBT/Fahr
10	79	M	PD	0	>20 yr	(–)	PD
11	77	M	PD	0	>1 yr	(–)	PD
12	84	M	MCI	0.5	(–)	2 yr	Early DLBT?
13	80	F	Unremarkable	0	(–)	(–)	CVD
14	90	F	Senile dementia	1	(–)	0.5 yr	AD/ CS
15	86	F	Unremarkable	0	(–)	(–)	Unremarkable
16	90	F	Senile dementia	1	(–)	>2 yr	DG
17	79	F	FTD	2	(–)	14 yr	AD
18	80	F	Dysphagia	0	(–)	(–)	Lewy body dysphagia
19	86	M	CBD	3	3 yr	n.d.	PSP
20	48	M	Unremarkable	0	(–)	(–)	Unremarkable

Abbreviations: CDR, clinical dementia rating (26) before suffering from terminal illness; PA, duration of Parkinsonism; Dementia, duration of dementia; yr, year; n.d., duration not determined due to unclear onset; PD, Parkinson disease; AD, Alzheimer disease; DLB, dementia with Lewy bodies; DLBN, DLB neocortical form (diffuse Lewy body disease); DLBT, DLB transitional form (limbic form); FTD, fronto-temporal dementia; MCI, mild cognitive impairment; CBD, corticobasal degeneration; CVD, cerebrovascular disease; N/A, not available; NFTD, neurofibrillary tangle-predominant form of dementia; CS, cervical spondylotic myelopathy; CVD, cerebrovascular disease; DG, dementia with grains; PSP, progressive supranuclear palsy; VD, vascular dementia of Binswanger type.

immunohistochemistry. Lewy dots outnumbered Lewy threads, making it unlikely that Lewy dots were simply cross sections of Lewy threads. The functional significance of these psyn-positive structures is open to speculation. Lewy dots and threads accompanied the cortical spongiosis associated with DLB, raising the possibility that they may disrupt synaptic transmission. The anti-psyn-immunoreactive axons in the affected limbic system suggest a possible disruption of axonal transport in LB-related cognitive decline. The presence of psyn-positive structures in the molecular layer of the occipital cortex in DLB neocortical form suggests a cause for the decreased uptake noted in occipital cortex with single photon emission computed tomography (SPECT) and fluor-deoxy-glucose positron emission tomography (PET) studies of DLB (19, 20).

Our study confirmed that α-synucleinopathy may start in the medulla oblongata, as previously reported by Del Tredici (9). However, in 5 of 15 AD cases, the process appeared to start in the amygdala at Stage 0.5 and then progressed to mildly involve the brainstem in Stage II. These findings suggest that there are 2 types of LB-related α-synucleinopathy: a primary type that starts in the medulla oblongata, and a secondary type that starts in the

amygdala. The primary type appears to progress into Parkinson disease and then DLB transitional form. The secondary type is associated with AD and possibly other tauopathies (21, 22), as was suggested by the association of one of our cases with PSP. The relation between DLB neocortical form and these primary and secondary types of α-synucleinopathy remains to be clarified.

Neostriatal pathology was reported with allosteric form-specific anti-α-synuclein antibody (23) and was confirmed by our anti-psyn immunocytochemistry. We observed numerous Lewy dots in a ventrolateral to dorsomedial gradient, consistent with the progression of Parkinson disease reported in a dopamine PET and biochemical study (24). The epitope of psyn was colocalized within plaques in dystrophic neurites or cores exclusively in some cases above Stage II. The possible association of Aβ and psyn deserves further study.

Our study showed that the neuropil pathology visualized with anti-psyn antibody was more widespread than reported previously. The observation that the presence of LBs was always accompanied by abundant neuropil pathology in the background supports the validity of the diagnostic criteria of DLB based on the LB score adopted

TABLE 2B
Neuropathological Summary of the Cases with Phosphorylated α-Synuclein-Related Neuronal Degeneration

Case	Stage	Score	tENT	Ci	F	T	P	O	NFT	SP
1	V	10 (10)	2 (2)	2 (2)	2 (2)	2 (2)	2 (2)	1	III	C
2	V	10 (9)	2 (2)	2 (2)	2 (2)	2 (2)	2 (1)	1	III	C
3	V	10 (8)	2 (2)	2 (2)	2 (1)	2 (2)	2 (1)	1	II	B
4	V	10 (9)	2 (2)	2 (2)	2 (2)	2 (2)	2 (1)	1	I	B
5	IV	10 (7)	2 (2)	2 (2)	2 (1)	2 (2)	2 (0)	1	I	B
6	IV	10 (7)	2 (2)	2 (2)	2 (1)	2 (2)	2 (0)	2	IV	B
7	IV	10 (7)	2 (2)	2 (2)	2 (1)	2 (2)	2 (0)	1	I	B
8	IV	10 (6)	2 (2)	2 (2)	2 (0)	2 (2)	2 (0)	1	I	A
9	IV	10 (6)	2 (2)	2 (2)	2 (0)	2 (2)	2 (0)	1	I	A
10	III	10 (6)	2 (2)	2 (2)	2 (0)	2 (2)	2 (0)	0.5	III	0
11	III	10 (6)	2 (2)	2 (2)	2 (0)	2 (2)	2 (0)	0.5	I	0
12	IIN	8 (6)	2 (2)	2 (2)	1 (0)	2 (2)	1 (0)	0.5	I	B
13	IIN	10 (8)	2 (2)	2 (2)	2 (0)	2 (2)	2 (1)	1	I	C
14	IIN	9 (5)	2 (2)	2 (1)	1 (1)	2 (0)	2 (1)	0.5	V	C
15	IIN	8 (5)	2 (2)	2 (2)	1 (0)	2 (1)	1 (0)	0	I	B
16	IIN	9 (6)	2 (2)	2 (1)	1 (0)	2 (2)	2 (1)	0.5	III	B
17	IIL	6 (2)	2 (0)	2 (1)	0 (0)	2 (1)	0 (0)	0	V	C
18	IIL	5 (3)	2 (1)	1 (1)	0 (0)	2 (1)	0 (0)	0	III	B
19	IIL	5 (0)	2 (0)	1 (0)	0 (0)	2 (0)	0 (0)	0	III	0
20	IIL	4 (0)	2 (0)	1 (0)	0 (0)	1 (0)	0 (0)	0	I	0

Scoring for Lewy bodies (score, tENT, Ci, F, T, and P) was assessed in sections immunostained for phosphorylated α-synuclein (psyn), following the consensus guidelines for dementia with LBs (6). The score in parentheses was determined by H&E staining and ubiquitin immunostaining. The score for Lewy bodies in the occipital cortex was determined by immunostaining for phosphorylated α-synuclein. Scores 0, 1, and 2 followed the consensus guidelines for dementia with LBs (6); the score 0.5 indicated Lewy threads and dots without intraneuronal perikaryal inclusions.

Abbreviations: NFT, neurofibrillary tangles, Braak staging (27); SP, senile plaque, Braak staging (27); Stage, Lewy body stage; Score, Lewy body score following consensus guidelines for dementia with LBs (6); tENT, transentorhinal area; Ci, cingulate gyrus; F, frontal lobe; T, temporal lobe; P, parietal lobe; O, occipital lobe.

by the consensus guidelines (6). The presence of widespread neuropil pathology is also consistent with previous reports that a decline of choline acetyl transferase (ChAT) is linearly correlated with the number of cortical LBs in the temporal neocortex (25).

Anti-psyn immunocytochemistry was too sensitive for assessment of Lewy scores using traditional criteria, making it necessary for us to adopt revised criteria. In our study, neocortical involvement was definitely present in the medial temporal lobe in Parkinson disease, spread to the frontal lobe in DLB transitional form, and additionally involved the parietal and occipital lobes in DLB neocortical form. This progressive involvement of the neocortex suggests that a revision of the diagnostic guidelines for LB-related cognitive decline may be warranted.

REFERENCES

1. Kuzuhara S, Mori H, Izumiyama N, Yoshimura M, Ihara Y. Lewy bodies are ubiquitinated. A light and electron microscopic immunocytochemical study. Acta Neuropathol (Berl) 1988;75:345–53
2. Spillantini MG, Schmidt ML, Lee VM, Trojanowski JQ, Jakes R, Goedert M. α-Synuclein in Lewy bodies. Nature 1997;388:839–40
3. Baba M, Nakajo S, Tu PH, et al. Aggregation of α-synuclein in Lewy bodies of sporadic Parkinson's disease and dementia with Lewy bodies. Am J Pathol 1998;152:879–84
4. Iwanaga K, Wakabayashi K, Yoshimoto M, et al. Lewy body-type degeneration in cardiac plexus in Parkinson's and incidental Lewy body diseases. Neurology 1999;52:1269–71
5. Jackson M, Lennox G, Balsitis M, Lowe J. Lewy body dysphagia. J Neurol Neurosurg Psychiatry 1995;58:756–58
6. McKeith IG, Galasko D, Kosaka K, et al. Consensus guidelines for the clinical and pathologic diagnosis of dementia with Lewy bodies (DLB): Report of the consortium on DLB international workshop. Neurology 1996;47:1113–24
7. Lennox GG, Lowe J. Dementia with Lewy bodies. In: Markesbery WR, ed. Neuropathology of dementing disorders. London: Arnold, 1998:181–92
8. Esiri MM, McShane RH. Parkinson's disease and dementia. In: Esiri MM, Morris JH, eds. The neuropathology of dementia. Cambridge: Cambridge University Press, 1997:174–93

9. Del Tredici K, Rub U, De Vos RA, Bohl JR, Braak H. Where does Parkinson disease pathology begin in the brain? J Neuropathol Exp Neurol 2002;61:413–26

10. Lippa CF, Fujiwara H, Mann DM, et al. Lewy bodies contain altered α-synuclein in brains of many familial Alzheimer's disease patients with mutations in presenilin and amyloid precursor protein genes. Am J Pathol 1998;153:1365–70

11. Arai Y, Yamazaki M, Mori O, Muramatsu H, Asano G, Katayama Y. α-Synuclein-positive structures in cases with sporadic Alzheimer's disease: Morphology and its relationship to tau aggregation. Brain Res 2001;888:287–96

12. Jakes R, Spillantini MG, Goedert M. Identification of two distinct synucleins from human brain. FEBS Lett 1994;345:27–32

13. Fujiwara H, Hasegawa M, Dohmae N, et al. α-Synuclein is phosphorylated in synucleinopathy lesions. Nat Cell Biol 2002;4:160–64

14. Saito Y, Nakahara K, Yamanouchi H, Murayama S. Severe involvement of ambient gyrus in dementia with grains. J Neuropath Exp Neurol 2002;61:789–96

15. McKeith IG, Perry EK, Perry RH. Report of the second dementia with Lewy body international workshop: Diagnosis and treatment. Consortium on Dementia with Lewy Bodies. Neurology 1999;53:902–5

16. Hasegawa M, Fujiwara H, Nonaka T, et al. Phosphorylated α-synuclein is ubiquitinated in α-synucleinopathy lesions. J Biol Chem 2002;277:49071–76

17. Kato T, Hirano A, Weinberg MN, Jacobs AK. Spinal cord lesions in progressive supranuclear palsy: Some new observations. Acta Neuropathol (Berl) 1986;71:11–14

18. Braak H, Braak E. Argyrophilic grains: Characteristic pathology of cerebral cortex in cases of adult onset dementia without Alzheimer changes. Neurosci Lett 1987;76:124–27

19. Ishii K, Yamaji S, Kitagaki H, Imamura T, Hirono N, Mori E. Regional cerebral blood flow difference between dementia with Lewy bodies and AD. Neurology 1999;53:413–16

20. Imamura T, Ishii K, Sasaki M, et al. Regional cerebral glucose metabolism in dementia with Lewy bodies and Alzheimer's disease: A comparative study using positron emission tomography. Neurosci Lett 1997;235:49–52

21. Forman MS, Schmidt ML, Kasturi S, Perl DP, Lee VM, Trojanowski JQ. Tau and α-synuclein pathology in amygdala of Parkinsonism-dementia complex patients of Guam. Am J Pathol 2002; 160:1725–31

22. Saito Y, Kawai M, Inoue K, et al. Widespread expression of α-synuclein and tau immunoreactivity in Hallervorden-Spatz syndrome with protracted clinical course. J Neurol Sci 2000;177:48–59

23. Duda JE, Giasson BI, Mabon ME, Lee VMY, Trojanowski JQ. Novel antibodies to synuclein show abundant striatal pathology in Lewy body disease. Ann Neurol 2002;52:205–10

24. Piggott MA, Marshall EF, Thomas N, et al. Striatal dopaminergic markers in dementia with Lewy bodies, Alzheimer's and Parkinson's diseases: Rostrocaudal distribution. Brain 1999;123:1449–68

25. Perry EK, Haroutunian V, Davis KL, et al. Neocortical cholinergic activities differentiate Lewy body dementia from classical Alzheimer's disease. Neuroreport 1994;5:747–49

26. Hughes CP, Berg L, Danziger WL, Coben LA, Martin RL. A new clinical scale for the staging of dementia. Br J Psychiatry 1982; 140:566–72

27. Braak H, Braak E. Neuropathological stageing of Alzheimer-related changes. Acta Neuropathol (Berl) 1991;82:339–59